Fusion Engineering and Design 112 (2016) 162–168

Contents lists available at ScienceDirect

Fusion Engineering and Design

journal homepage: www.elsevier.com/locate/fusengdes

Numerical and experimental characterization of ceramic pebble beds under cycling mechanical loading

S. Pupeschi[a,*], R. Knitter[a], M. Kamlah[a], Y. Gan[b]

[a] Institute for Applied Materials, Karlsruhe Institute of Technology (KIT), Germany
[b] School of Civil Engineering, The University of Sydney, Sydney, NSW, 2006, Australia

HIGHLIGHTS

- The effect of cyclic loading on the mechanical response of pebble beds was assessed.
- Numerical simulations were performed with KIT-DEM code.
- The numerical simulations were compared with the experimental outcomes.
- A good qualitative agreement between experimental and simulation results was found.
- The pebble size distribution affects the mechanical response of the assemblies.

ARTICLE INFO

Article history:
Received 18 April 2016
Received in revised form 17 August 2016
Accepted 18 August 2016

Keywords:
Discrete element method
Pebble beds
Numerical simulation
Granular materials
Breeder blankets
Ceramic breeder

ABSTRACT

All solid breeder concepts considered to be tested in ITER (International Thermonuclear Experimental Reactor), make use of lithium-based ceramics in the form of pebble-packed beds as tritium breeder. A thorough understanding of the thermal and mechanical properties of the ceramic pebble beds under fusion relevant conditions is essential for the design of the breeder blanket modules of future fusion reactors. In this study, the effect of cyclic loading on the mechanical behaviour of pebble bed assemblies was investigated using a Discrete Element Method (DEM) code. The numerical simulations were compared with the experimental outcomes. The results of numerical simulations show that the pebble size distribution affects noticeably the stress-strain behaviour of the assemblies. A good qualitative agreement between experimental and simulation results was found in terms of difference between residual strains of consecutive cycles. An increase of the oedometric modulus with the compressive load was observed for all investigated compositions in both experimental and DEM simulations. The numerical results show an increase of the oedometric modulus (E) with progressive compaction of the assemblies due to the cycling loading, while no significant influence of the pebbles size distribution was observed.

1. Introduction

A tritium Breeding Blanket (BB), ensuring tritium breeding self-sufficiency, is a compulsory component for the DEMOnstration Power Plant (DEMO). Presently, two tritium breeder concepts (solid breeder blanket and liquid metal breeding blanket) are considered to be tested in the International Thermonuclear Experimental Reactor (ITER). In the solid breeder blanket concept, the ceramic breeding material is in the form of pebble-packed beds. The present reference tritium breeding material for the European Helium Cooled Pebble Bed (HCPB) breeder blanket concept consists of a two-phase material (Li_4SiO_4 + 10mol% Li_2SiO_3) [1]. In 2009 an Advanced Ceramic Breeder (ACB) material was proposed [2], to optimize the mechanical stability of lithium orthosilicate pebbles lithium metatitanate was introduced as a second phase. Even if the ceramic beds have no structural function, the beds have to withstand stresses induced by the blanket operating conditions. A blanket module will experience a cycling loading due to the burn pulses of the plasma. Due to the temperature gradients and a mismatching of the thermal expansion coefficients between the beds and the structural materials, a cyclic compressive load will arises on the beds.

An experimental set-up for the investigation of the effective thermal conductivity of ceramic pebble beds was designed and assembled [3]. The hot wire method was selected to measure the thermal conductivity of ceramic pebble beds [4]. During the

* Corresponding author.
E-mail address: pupeschi.simone@hotmail.it (S. Pupeschi).

http://dx.doi.org/10.1016/j.fusengdes.2016.08.021
0920-3796/

experimental campaign simultaneous measurements of the thermal conductivity and stress-strain properties were conducted.

Discrete element methods (DEM) have been adopted previously to study the thermo-mechanical responses of pebble bed assemblies [5–7]. An in-house DEM code [8] was successfully used in previous studies [8,9] to investigate the mechanical behaviour of mono-sized, binary and polydispersed pebble assemblies. In these simulation studies a defined uni-axial macroscopic strain (ε_{33}) was gradually applied on random pebble assemblies. When the defined maximum strain was reached, the assemblies were unloaded by gradually removing ε_{33} until the stress σ_{33} approaches zero. No repeating cycles were simulated; the studies were focused on the first loading/unloading cycle.

A recent research [10] investigated the effect of mechanical cycling on the behavior of granular materials. The simulations were carried out with an assembly consisting of mono-size spherical pebbles (diameter of 0.5 mm) with an initial packing factor (PF) of 59.9%. The pebbles were randomly generated in a cubic box made of steel. The bed was compressed imposing a cyclic loading on the top wall of the box, the number of compressive load was limited to 10 cycles. The initial packing factor used in the study is actually below the reference value for the solid BB concept. Furthermore, in the EU solid BB concept, polydispersed beds are used.

Zhang et al. [11] recently investigated the stability of pebble beds under pulsed loading conditions. Both Uniaxial Compression Tests (UCTs) and Finite Element Method (FEM) simulations were conducted. The UCTs were performed at elevated temperatures (up to 750 °C) on both the EU Ref. [1] (PF = 61%) and Li_2TiO_3 [12] (PF = 63%) tritium breeding materials. The FEM simulations were carried out to study the coupled thermo-mechanical problem of HELICA mock-up experiment [13].

In this study, the in-house DEM code developed in [8] was used to investigate the influence of cyclic loading on the mechanical behavior of polydispersed pebble bed assemblies with periodic boundary conditions. To provide a representative result for the EU BB, an initial PF of approx. 64% was used. The results were compared with the experimental outcomes of the UCTs, conducted at room temperature, performed during the thermal conductivity experimental campaign.

2. Experimental

Fig. 1 shows the developed experimental set-up for the measurements of ceramic pebble beds' thermo-mechanical properties [3]. The experimental set-up was designed for the investigation of ceramic pebble beds' thermal conductivity as a function of temperature, mechanical load and filling gas type/pressure. Simultaneous measurements of the thermal conductivity and stress-strain properties were conducted. Even if the bed deformation (mm) is measured during the experiments at each investigated temperature, the evaluation of the bed strain ε (%) is only possible at room temperature when the initial bed height is known. For that reason the results of the simulations were compared with experiments at RT.

A cylindrical measuring cell of 55 mm inner diameter with the heater placed along its axis is filled by ceramic pebbles. Pebbles were packed into the measuring cell by mechanical vibration; the initial PF of the beds was approx. 64% with an initial height of approx. 40 mm. The experimental set up is placed axially on a universal testing machine; the pebble bed is compressed up to 6 MPa in the axial direction by a piston connected to the movable crossbar of the testing machine. The bed was compressed five times with a loading/unloading speed of 1 MPa/min. The lateral displacement of the pebble bed is inhibited by the measuring cell while the axial strain arises by applying the vertical load. The bed strain is measured by means of three linear variable displacement transducers (LVDT) equally spaced with 120° along the poloidal direction while the compressive load is measured by a load cell.

Polydispersed lithium orthosilicate pebble beds characterized by different pebble size distributions and different Lithium metatitanate (LMT) contents were examined. The investigated ACB compositions [2] were:

- 20 LMT → Li_4SiO_4 + 20 mol% Li_2TiO_3
- 25 LMT → Li_4SiO_4 + 25 mol% Li_2TiO_3
- 30 LMT → Li_4SiO_4 + 30 mol% Li_2TiO_3

The EU reference (EU Ref.) tritium breeding material (Li_4SiO_4 + 10 mol% Li_2SiO_3), fabricated by Schott AG by the melt-spraying method [14], was investigated as well. Pebbles fabricated by this method are characterized by a peaked pebble size distribution in the range 0.25-0.65 mm. The lithium orthosilicate pebbles with LMT as a second phase have been fabricated at KIT by a melt-based process [15]. In Fig. 2, the pebble size distributions of the four investigated compositions are reported. As shown in the figures, pebbles fabricated by the melt-based process are characterized by broader pebble size distributions in the range 0.25-1.25 mm. Among the ACB materials, the pebble size distribution of 20LMT is more representative of a typical batch produced by the melt-based process (Fig. 2b). The pebble size distributions of 25 and 30 LMT (Fig. 2c and d) are not typically obtained by the production process but selected here to have a set of distinct assemblies, representative of a more uniform distribution.

Approximately 150 g of pebbles were used for each experiment. Before using, the pebbles were dried at 300 °C for one hour in a vacuum oven. The experiments were carried out in helium atmosphere. The physical characteristics of the studied pebbles are given in Table 1.

3. Numerical simulations

In this study, the existing in-house DEM code [8] was slightly modified in order to simulate cyclic loading with the stress σ_{33} as the driven parameter. The simulated assemblies consist of 5000 spherical pebbles packed in periodic configuration into a virtual cubic box. Using, in addition, periodic boundary conditions, we represent the bulk behaviour of the pebble beds and avoid friction effects and the impact on the packing factor due to the presence of container walls. The assemblies were generated using a Random Close Packing (RCP) algorithm [16] with a PF of approx. 64%, consistent with the reference value of the actual EU BB design. The assemblies were generated with the actual pebble size distributions of the EU Ref. and of the three modified breeder ceramic compositions, respectively. For each investigated composition an assembly with a PF close to the experimental value was created. The assemblies were subjected to cyclic loading simulating the experimental uni-axial compression tests. Starting from the stress-free configuration, generated by the RCP algorithm, the assemblies were progressively loaded up to a defined maximum stress ($\sigma_{33} = \sigma_{max}$). After the loading, the assemblies were unloaded by gradually reducing σ_{33} until the stress-free configuration, $\sigma_{33} \approx 0$, was reached. As in the experiments the assemblies were compressed by five loading cycles.

Furthermore, for the assembly simulating 20 LMT, representative of the size distribution for the melt-based process, another assembly with a PF of approx. 64% was created. The loading/unloading process was repeated 30 times, this time. Three maximum loads of 6, 4 and 2 MPa were applied. The performed simulations are listed in Table 2. The sample ID reported in the table

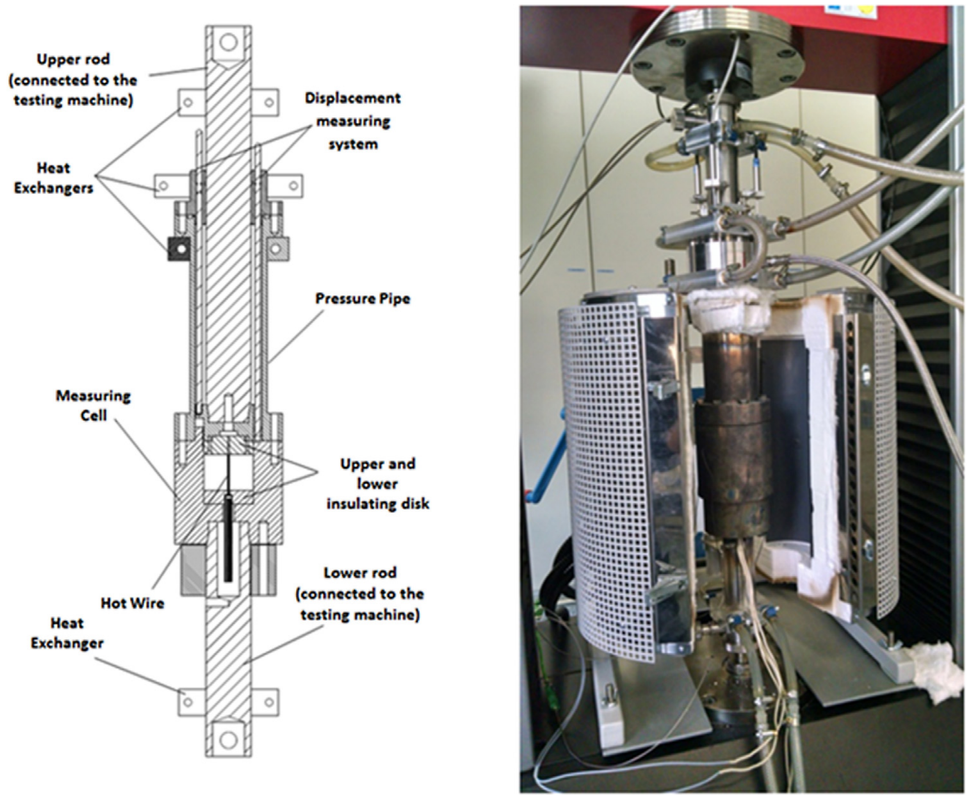

Fig. 1. Experimental set-up for the measurements of ceramic pebble beds' thermal conductivity.

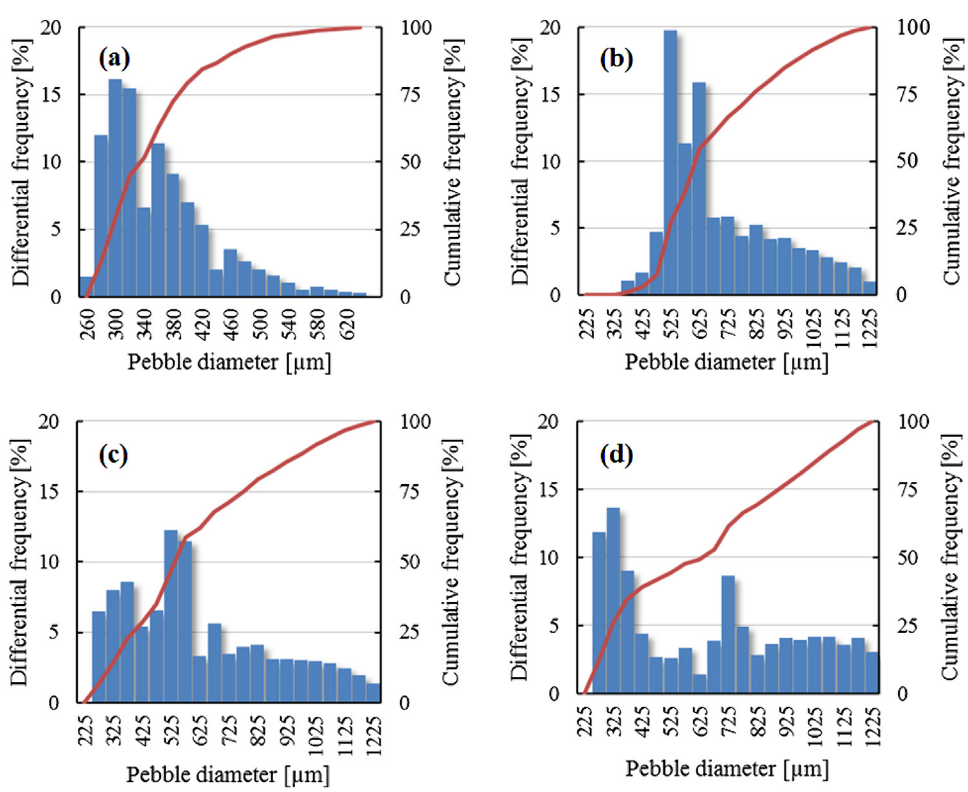

Fig. 2. Size distributions of (a) EU Ref., (b) 20LMT, (c) 25LMT, and (d) 30LMT pebbles.

Table 1
Characteristics of the investigated materials.

ID	Material	Density(g/cm^3)	Pebble diameter(mm)	Density(% th. density)	Packing factor(%)
20LMT	Li_4SiO_4 + 20 mol% Li_2TiO_3	2.54	0.25–1.25	93.0	64.2
25LMT	Li_4SiO_4 + 25 mol% Li_2TiO_3	2.58	0.25–1.25	93.3	64.2
30LMT	Li_4SiO_4 + 30 mol% Li_2TiO_3	2.62	0.25–1.25	93.5	64.2
EU Ref.	Li_4SiO_4 + 10 mol% Li_2SiO_3	2.40	0.25–0.65	95.1	64.1

Table 2
Performed simulations.

ID	No. Loading cycles	PF (%)	Max. load [MPa]
20LMT-30-6	30	64.056	6
20LMT-30-4			4
20LMT-30-2			2
20LMT-5	5	64.225	6
25LMT-5	5	64.226	6
30LMT-5	5	64.246	6
EU Ref.-5	5	64.154	6

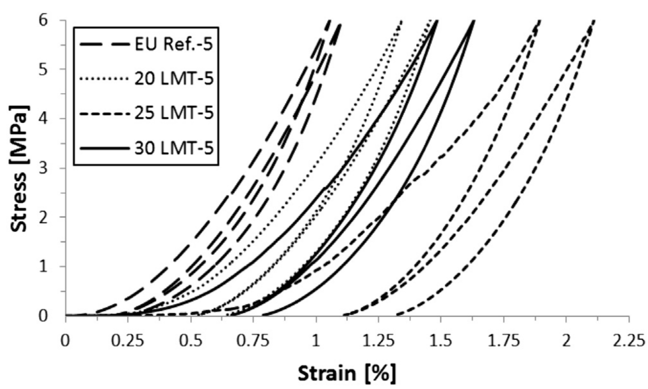

Fig. 3. Simulated stress-strain curves of the investigated compositions for the 1 st and the 2 nd loading/unloading cycle.

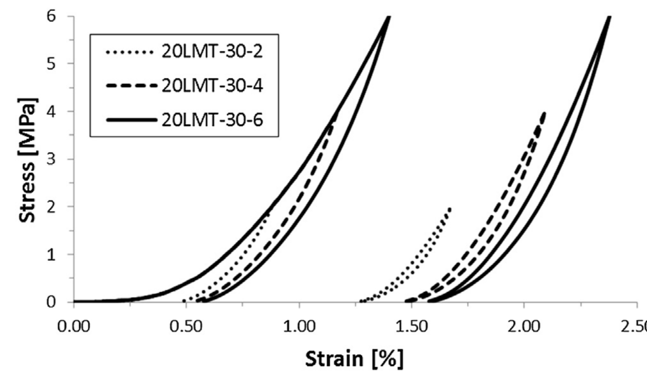

Fig. 4. Simulated stress-strain curves for the 1 st and the 30th loading/unloading cycles with different maximum compressive load.

signifies the investigated material, the number of loading cycles and maximum load.

Due to lack of experimental data, the mechanical properties of EU Ref. were used for all investigated assemblies. A Young's modulus of (E) equal to 90 GPa and a Poisson's ratio (ν) equal to 0.25 were used. The friction coefficient between pebbles (μ) was set to 0.1. The mechanical behaviour of pebble beds subjected to cyclic loads at high temperatures was not addressed due to a lack of material properties data at high temperatures. All mechanical properties available refer to room temperature.

4. Results and discussion

Fig. 3 shows the simulated stress-strain curves of the investigated assemblies subjected to five compressive cycles. In the graph only the first two loading/unloading cycles are reported (so that figure is not overloaded by curves plotted on top of each other). As shown in the figure, the size distribution influences the stress-strain behaviour of the assemblies. Even though the EU reference breeding material has the lowest PF, it shows the stiffer behaviour (smaller strain for a given stress) with a residual strain less than 0.2% after the first unloading. This assembly is characterized by a narrow and peaked size distribution resulting, for the given PF, in a denser configuration in comparison to the ACB materials. The assemblies representing the modified breeder compositions show a softer behaviour compared to the reference breeding material. Furthermore, even if the three assemblies have the same size ranges, differences in the overall stress-strain behaviour due to the different pebble size distributions were observed. In particular, the stiffer behaviour with the lower residual strain after the first unloading refers to 20 LMT, which shows a peaked pebble size distribution around 575 μm. Samples with 25 and 30 LMT are characterized by a smoother pebble size distribution resulting in a softer stress-strain behaviour. In particular 25 LMT deforms significantly (approx. 0.4%) before the stress is build up.

In Fig. 4 the simulated stress-strain curves of 20LMT-30 with a maximum compressive load of 6, 4 and 2 MPa are reported. For this assembly 30 loading/unloading cycles were simulated, in the figure only the first and the last cycles are shown. An increase of the total residual strain with increasing maximum compressive load was observed. Because of the greater perturbation provided to the system, the residual strain of the bed is more pronounced with higher loads than with smaller loads (higher contact forces are induced leading to overcome the friction between pebbles).

The results of the simulations were compared with the experimental outcomes in terms of difference between residual strains of two consecutive cycles and calculated oedometric modulus. The difference between the residual strains of two consecutive cycles represents the increment of the irreversible residual strain due to the cycling loading. The experimental and simulated stress-strain curves were not directly compared because the first loading/unloading cycle sensitively depends on the initial PF and on the first approach of the piston to the pebble bed. Previous studies [8,9] showed that the initial PF plays an important role in the mechanical response of an assembly in both experimental and DEM simulations. The experimental PF is an average of bulk and near wall regions PFs while the DEM assembly represents the bulk region of a pebble bed, because of the periodic boundary conditions. Moreover, a quantitative comparison with experimental data in terms of stress-stain curves, even after the second cycle onwards, cannot be made. The experimental curves show a stiffer behaviour while a more compliant response is observed for the simulations. This is due to the differences that exist between simulations and experimental conditions. In particular to the H/D ratio adopted in the UCTs and to the friction coefficient between pebbles used in the simulations (later discussed in the paper). In the present paper the attention was then focused on the engineering parameters needed for the design of the solid breeder blanket concept.

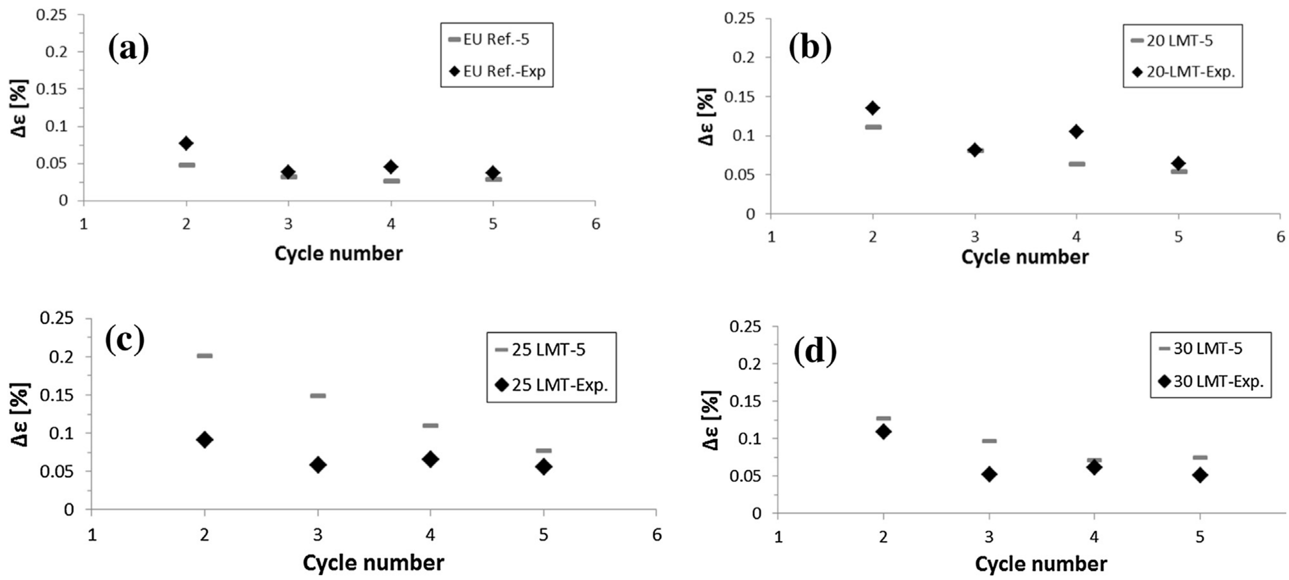

Fig. 5. Difference between the residual strains of two consecutive cycles of (a) EU Ref., (b) 20LMT, (c) 25LMT, and (d) 30LMT.

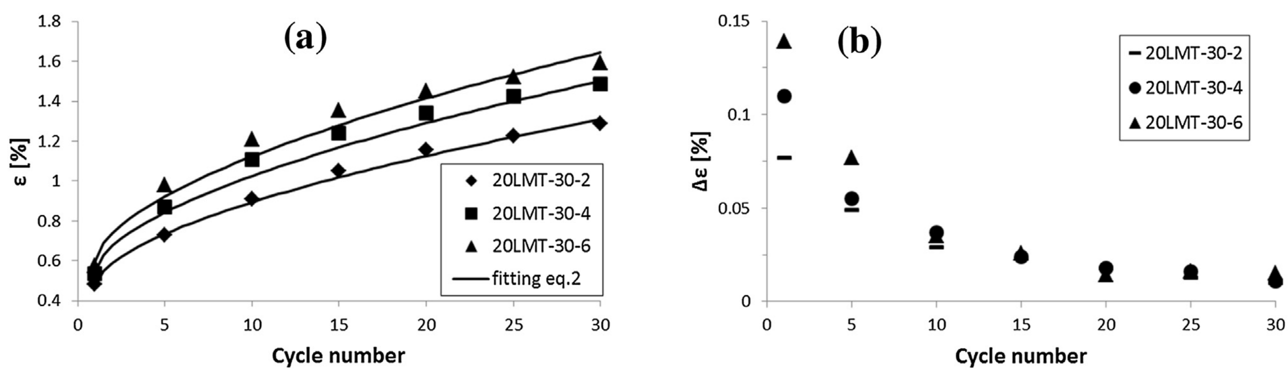

Fig. 6. Residual strain as a function of the cycle number (a) and difference between the residual strains of two consecutive cycles (b) of 20 LMT-30.

In Fig. 5, the difference between the residual strains of two consecutive cycles are reported and compered with experimental values. The residual strain after the first loading cycle is omitted. A good qualitative agreement between experiments and simulations was found, as the progressive compaction of the bed due to the cyclic loading is clearly shown. In particular the EU Ref. shows a smaller difference between the residual strains of two consecutive cycles, evidence of the more dense structure developed in this material, which is closer to its maximum PF than in case of ACB materials.

In Fig. 6, the residual strain and the difference between the residual strains of two consecutive cycles as a function of the cycle number of 20LMT-30 are reported. As shown in the figure, the largest part of the irreversible residual strain occurs during the first 15 cycles, while the compaction of the assembly is still progressing but with smaller increments as the cycling proceeds. In terms of difference between the residual strains of two consecutive cycles the maximum compressive load affects the first 5 cycles. Similar results were reported in [10] and [11]. However, quantitative comparisons cannot be made because of the different pebble size and boundary conditions used.

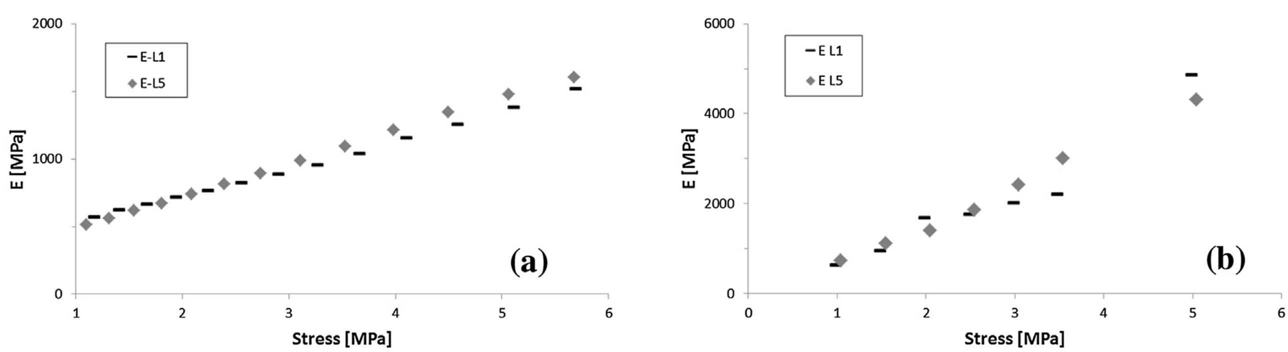

Fig. 7. Calculated oedometric moduli derived from (a) the simulated and (b) the experimental stress-strain curves.

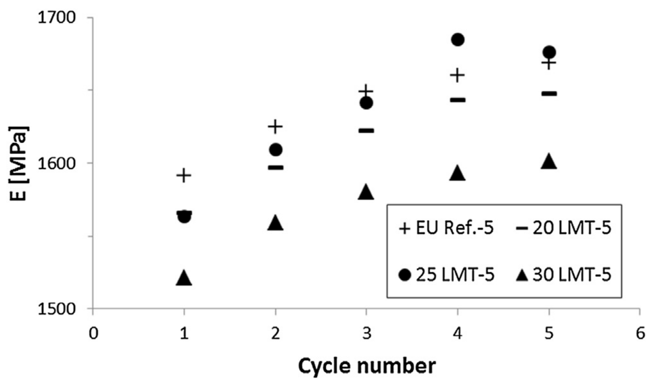

Fig. 8. Increase of the oedometric modulus upon unloading with the cycle number derived from simulations.

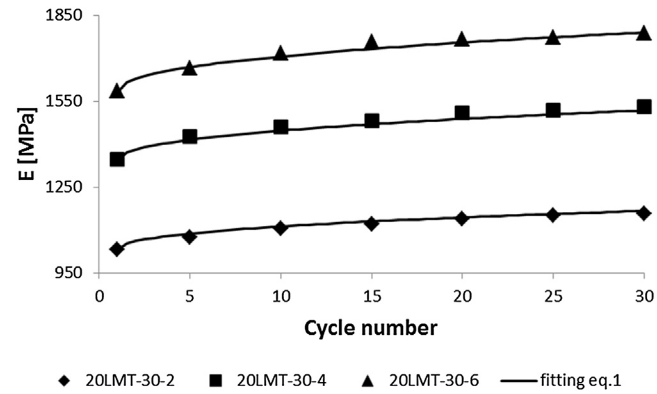

Fig. 9. Increase of the oedometric modulus upon unloading with the cycle number for 20 LMT-30 derived from simulations.

Fig. 7 exemplarily displays the calculated oedometric moduli derived from the experimental and from the simulated stress-strain curves. In the figures the oedometric moduli of 30LMT are reported as a function of the compressive load. The oedometric modulus (E) was calculated as $E = \frac{\Delta\sigma}{\Delta\varepsilon}$ during the unloading. *E-L1* and *E-L5* in the figures refer to the oedometric modulus calculated for the first and the fifth unloading, respectively.

An increase of E with the compressive load was observed for all investigated compositions in both experimental and DEM simulations, however higher values of E were obtained from the experimental data, as compared to the simulation results. This reflects the more compliant mechanical response observed for the simulated curves. The stress-strain behaviour obtained by the uni-axial compression test is influenced by the ratio H/D [17]. As reported before, the experimental data refer to a 40 mm high pebble bed with a diameter of 55 mm (H/D = 0.73). The current bed height of 40 mm is a compromise for a reliable measurement of the thermal conductivity with a uniform compressed bed along its axis. A higher value of the bed height would be beneficial for the thermal conductivity measurement, but detrimental to the uniformity of the mechanical compression. Indeed, increasing the bed height, the effective constrains at the cylindrical wall increases and may introduces arching of pebbles inside the container, reducing the actual pressure in the bed with increasing axial distance from the piston, resulting in a bed compressed only in the upper part [17]. As reported in [17] the wall friction, which is directly related to the ratio H/D, affects the steepness of the unloading curve leading to higher values of E compared to the simulations, in which the friction between the boundaries and pebbles was not considered. Furthermore, due to the lack of experimental data, an arbitrary friction coefficient between pebbles equal to 0.1 was used. As reported in [9] the friction coefficient can have profound influence on the stress–strain response of the assembly. For these reasons quantitatively comparisons between experimental and simulations results on the calculated elastic constants cannot be made.

In Fig. 8, the oedometric moduli upon unloading of the simulated assemblies as a function of the cycle number are reported. In agreement with [10] the numerical results show an increase of E with the progressive compaction of the assemblies due to the cycling loading, the increase falls between 5% and 7%. As shown in the figure no significant influence of the pebble size distribution of the assembly was observed, the maximum difference between the assemblies after five cycles is about 5%.

In Fig. 9, the calculated oedometric moduli upon unloading of 20LMT-30 as a function of the cycles for compressive loads of 6, 4 and 2 MPa are displayed. An increase of E with increasing maximum compressive load was observed. The higher compressive load leads to a higher ability of the pebbles to move in the structure, resulting in a denser packing structure of the assembly (higher PF) than in the assemblies subjected to a lower compressive load. As reported before, an increase of E with the progressive compaction of the assemblies was observed due to the cycling loading. More cycles were simulated for this assembly, and we observe that E is increasing rapidly during the first 10–15 cycles and it tends to saturate afterwards. Of a total observed increment of about 13% after 30 cycles, an increase of approx. 10% was already observed after 15 cycles.

Table 3
Numerical coefficients.

Max. load [MPa]	E_1 [MPa]	ε_1 [%]
2 MPa	1030	0.47
4 MPa	1340	0.54
6 MPa	1580	0.59

The following correlations, derived from the simulations (Fig. 6a and Fig. 9), are suggested for the estimation of E and ε of ceramic pebble beds as a function of cycle number (N) for compressive loads of 2, 4 and 6 MPa:

$$E_N\,[MPa] = E_1\left[0.031(N-1)^{0.434}+1\right] \tag{1}$$

$$\varepsilon_N\,[\%] = \varepsilon_1\left[0.025(N-1)^{0.583}+1\right] \tag{2}$$

Where E_1 is the oedometric modulus upon the first unloading while ε_1 is the residual strain after the first unloading. Since a good qualitative agreement between experiments and simulations was found in terms of difference between residual strains of consecutive cycles (Fig. 5), even taking into account all the differences between simulations and experiments., Eq. (2) can reasonably represent also the experimental results. The values of E_1 and ε_1 are reported in Table 3 for the investigated compressive loads.

5. Conclusions and future work

In this study, the effect of cyclic loading on the mechanical behaviour of pebble bed assemblies was investigated using an in-house DEM code. Four assemblies with different pebble size distributions were investigated. Results of numerical simulations show that the pebble size distribution affects the stress-strain behaviour of the assemblies. The assembly representing the EU reference breeding material, characterized by a narrow and peaked size distribution, shows a stiffer behaviour compared to the assemblies representing the modified breeder materials, characterized by a broader size distribution. The stiffer behaviour of the EU Ref. is an evidence of the more dense structure developed in this material, closer to the maximum theoretical PF than the ACB materials. In comparison, pebble beds characterized by a broader pebble size distribution can experience higher strains without building up stress at the beginning of loading.

Even if the simulated residual strain after the first unloading cannot be compared with the experimental one, mainly because of the uncertainty of the initial PF and of the first approach of the piston to the pebble bed, a good qualitative agreement between experiment and simulation results was found in terms of difference between residual strains of consecutive cycles even taking into account all the differences between simulations and experiments. The progressive compaction of the bed due to the cyclic loading is clearly shown. In agreement with [11], the first 10–15 cycles are responsible for the largest part of the irreversible residual strain. Afterwards, as the cycling proceeds, the compaction of the assembly is still progressing but with smaller increments. The maximum compressive load imposed on the bed affects the first 5 cycles. This means that increasing the imposed load leads to a higher irreversible strain during the first cycles as compared to a lower load. However, for the period following the first 5 cycles, the same increasing rate is reached at a lower compressive load. The EU Ref. material shows a smaller difference between the residual strains of two consecutive cycles, a confirmation of the fact that this material is closer to the maximum possible PF.

Because of the influence of the wall friction and the friction coefficient between pebbles, a quantitative comparison with experimental data in terms of stress-stain curve and calculated oedometric modulus cannot be made. An increase of the oedometric modulus with the compressive load was observed for all investigated compositions in both, the experiments and the DEM simulations. The results show no significant influence of the pebble size distributions on the oedometric modulus. An increase of E with increasing imposed compressive load was observed. The numerical results show an increase of E with progressive compaction of the assemblies due to the cycling loading. The simulations show that E is rapidly increasing during the first 10–15 cycles and tends to saturate afterwards. Even if similar results were obtained in [10] and [11], quantitative comparisons with the present study on the calculated elastic constants and the progressive compaction of the bed cannot be made, because of the different pebble size and boundary conditions used.

From the results of the simulations correlations for the estimation of E and ε of ceramic pebble beds as a function of the cycle number for maximum compressive loads of 2, 4 and 6 MPa were derived.

An experimental campaign aimed at the mechanical characterization of pebble beds is needed. In further experiments a lower H/D ratio of the bed will be used in order to reduce the influence of the wall friction and the influence of the near wall regions on the PF. The results will be compared with numerical simulations.

Acknowledgments

Part of this work was executed during a stay of S.P. at The University of Sydney with Y.G. Financial support by International Program Development Fund (IPDF) at The University of Sydney is gratefully acknowledged.

References

[1] R. Knitter, B. Löbbecke, Reprocessing of lithium orthosilicate breeder material by remelting, J. Nucl. Mater. 361 (2007) 104–111.
[2] R. Knitter, et al., Fabrication of modified lithium orthosilicate pebbles by additions of titania, J. Nucl. Mater. 442 (2013) S433–S436.
[3] S. Pupeschi, Study of thermal conductivity of ceramic pebble beds, EUROfusion (2014), 2M8Y29.
[4] K.D. Maglic, A. Cezairliyan, V. Peletsky, Compendium of Thermophysical Property Measurement Methods, 1, Plenum Press, New York, 1984, pp. 61–122.
[5] Z. An, et al., Numerical characterization of thermo-mechanical performance of breeder pebble beds, J. Nucl. Mater. 367–370 (2007) 1393–1397.
[6] Z. An, et al., Application of discrete element method to study mechanical behaviors of ceramic breeder pebble beds, Fusion Eng. Des. 82 (2007) 2233–2238.
[7] J.T. Van Lew, et al., A discrete element method study on the evolution of thermomechanics of a pebble bed experiencing pebble failure, Fusion Eng. Des. 89 (2014) 1151–1157.
[8] Y. Gan, M. Kamlah, Discrete element modelling of pebble beds: with application to uniaxial compression tests of ceramic breeder pebble beds, J. Mech. Phys. Solids 58 (2010) 129–144.
[9] R.K. Annabattula, et al., Mechanics of binary and polydispersed spherical pebble assembly, Fusion Eng. Design 87 (2012) 853–858.
[10] X. Wang, et al., Computational study on the behaviors of granular materials under mechanical cycling, J. Appl. Phys. 118 (2015) 174901.
[11] C. Zhang, et al., Ceramic breeder pebble bed packing stability under cyclic loads, Fusion Eng. Des. (2016), http://dx.doi.org/10.1016/j.fusengdes.2016.03.014.
[12] Yi-Hyun Park, et al., Fabrication of Li_2TiO_3 pebbles using PVA?boric acid reaction for solid breeding materials, J. Nucl. Mater. 455 (2014) 106–110.
[13] G. Dell'Orco, et al., Progress in the benchmark exercise for analyzing the lithiate breeder pebble bed thermo-mechanical behaviour, Fusion Eng. Des. 81 (2006) 169–174.
[14] W. Pannhorst, et al., Production process of lithium orthosilicate pebbles fusion technol, Sept. 7–11, 1998, Marseille, France, in: B. Beaumont, P. Libeyre, B. de Gentile, G. Tonon (Eds.), Proceedings of 20th Symposium on Fusion Technology, 2, 1998, pp. 1441–1444.
[15] M. Kolb, et al., Enhanced fabrication process for lithium orthosilicate pebbles as breeding material, Fusion Eng. Des. 86 (2011) 2148–2151.
[16] Y. Gan, et al., Computer simulation of packing structure in pebble beds, Fusion Eng. Des. 85 (2010) 1782–1787.
[17] J. Reimann, et al., Influence of pebble bed dimensions and filling factor on mechanical pebble bed properties, Fusion Eng. Des. 69 (2003) 241–244.